CEAS Space Journal (2025) 17:917–929
https://doi.org/10.1007/s12567-025-00601-2

ORIGINAL PAPER

Ferrofluid reaction wheel development and in-orbit verification

Manfred Ehresmann[1] · Sebastian Zajonz[2] · Christian Korn[2] · Steffen Großmann[2] · Janoah Dietrich[2] · Maximilian Kob[2] · Daniel Philipp[2] · Fabrizio Turco[2] · Michael Steinert[2] · Michael O'Donohue[2] · Nicolas Heinz[2] · Elizabeth Gutierrez[2] · Alexander Wagner[2] · Daniel Bölke[2] · Saskia Sütterlin[2] · Maximilian Schneider[2] · Yolantha Remane[2] · Phil Kreul[2] · Bianca Wank[2] · Manuel Buchfink[2] · Denis Acker[2] · Sonja Hofmann[2] · Bahar Karahan[2] · Silas Ruffner[2] · Felix Schäfer[1] · Georg Herdrich[1]

Received: 30 March 2024 / Revised: 3 February 2025 / Accepted: 4 February 2025 / Published online: 25 February 2025

Abstract

In contemporary satellite systems, the Attitude and Orbit Control System (AOCS) manages internal torque generation primarily through Reaction Wheels (RW) and Control Moment Gyros (CMG), which use mechanically mounted rotating disks to control orientation without expelling mass. Unlike magnetorquers, which interact with Earth's magnetic field, or thruster-based Reaction Control Systems (RCS), which generate external forces by expelling propellant, RW and CMG systems rely solely on momentum exchange within the spacecraft. While state-of-the-art RWs are highly reliable and have demonstrated exceptional performance over decades of operation, their design still presents inherent challenges, such as wear, nonlinear friction effects, and tribological degradation of contact surfaces. These challenges are critical in space, where repairs are impractical and/or resource-intense. Consequently, engineers have devoted significant effort to developing robust and reliable mechanical reaction wheels. This paper explores an innovative proof-of-concept design based on a fluid-magnetic system utilizing ferrofluids and permanent magnets. This study aims to address limitations of traditional RWs by eliminating mechanical interfaces susceptible to wear and tear and replacing them with a low friction ferrofluidic bearing. Ferrofluid-based system concepts can offer a longer life due to reduced wear and tear, lower production costs by requiring less exotic materials and tolerances, self-center within the provided magnetic potential field and can therefore exhibit reduced vibration behavior. The Ferrowheel experiment, flown as part of the FARGO mission (*Überflieger 2* competition of the space agency within DLR) in March and April 2023, demonstrated the feasibility of ferrofluidic bearings for attitude control in ISS microgravity. These results contribute to exploration of innovative reaction wheel technologies, highlighting the potential of fluid-based systems for applications requiring enhanced robustness and reduced mechanical wear.

Keywords FARGO · ISS · DLR · Ferrofluid · AOCS · Student project · Wear-reduction · Mechanic-free

Abbreviations

AC	Alternating current
AOCS	Attitude and orbit control system
BLDC	Brushless DC electric motor
CAD	Computer aided design
COTS	Commercial off-the-shelf
CMG	Control moment gyro
DC	Direct current
DLR	German aerospace center
ESC	Electronic speed controller
EMI	Electromagnetic interference
EMF	Electromotive force
FARGO	Ferrofluid application research goes orbital
FUSE	Far ultraviolet spectroscopic explorer
ICD	Interface control document
MoI	Moment of inertia
RPM	Revolutions per minute
RW	Reaction wheel
PC	Polycarbonate
PCB	Printed circuit board
PTFE	Polytetrafluoroethylene
RCS	Reaction control systems
STEM	Science, technology, engineering, maths

✉ Manfred Ehresmann
ehresmann@irs.uni-stuttgart.de

[1] Institute of Space Systems, University of Stuttgart, Pfaffenwaldring 29, 70569 Stuttgart, Germany

[2] FARGO Team Member, KSat e.V., Pfaffenwaldring 29, 70569 Stuttgart, Germany

1 Introduction

Space missions demand highly durable and reliable components, as in-orbit maintenance is often impractical, unfeasible or resource-intensive. Therefore, the durability and reliability of each space component used is crucial [1]. Mechanical systems with moving parts have the distinct challenge of being prone to wear and tear due to the inherent friction involved by solid-solid interfaces in relative motion, i.e. tribological effects. Therefore, critical engineering ensuring mission lifetime is needed or a maintenance need will inevitably arise if the component lifetime is exceeded. This leads to a hard trade-off between resource-intensive repairs, component replacement or redundancy. From the design point of view cost intensive high-quality materials, accepting reduced component life or accepting mission risk are possible trade-offs. Mechanical degradation is in principle inevitable for moving parts and its effects are particularly pronounced in Attitude and Orbit Control Systems (AOCS) [2].

Conventionally, most satellites and spacecraft use mechanical reaction control systems like reaction wheels (RW) or control moment gyros (CMG) for internal torque generation. For a reaction wheel system, a high MoI (Moment of Inertia) rotating disk is accelerated or decelerated via an electric motor usually by varying the rotation rate of the applied magnetic field.

Adjusting the rotation rate generates internal torque and transfers angular momentum, following the principle of momentum conservation, either to the flywheel or the satellite structure. These torque generation systems are crucial for compensating for attitude disturbances or for maintaining precise orientation to track the Sun, stars, or targets on Earth's surface. Common sources of attitude disturbances include solar radiation pressure, atmospheric drag, and the non-uniformity of Earth's gravity field.

Decades of critical engineering and analysis of in-orbit failures [3] have produced state-of-the-art reaction wheels that are generally considered highly reliable. For example, the Hubble Space Telescope underwent servicing missions STS-82 and STS-109, during which entire reaction wheel assemblies were replaced due to electrical anomalies requiring maintenance [4]. On Earth, analyses of in-space degradation have offered valuable insights for improving reaction wheel design and performance. Simultaneously, unreplaced reaction wheel assemblies aboard the Hubble have continued to function reliably, demonstrating exceptional longevity for well over three decades.

In April 2024, however, an issue arose with one of Hubble's gyroscopes [5]. These gyroscopes, part of the sensor package used for attitude determination, are fast-rotating devices operating on gas bearings at a constant rate. The relevance to this work lies in their mechanical challenges, particularly the "flex leads" that carry power and data but experience mechanical strain during nominal operations, making them susceptible to wear over time [6].

While reaction wheels are considered technologically mature, there are several notable missions where their performance posed challenges to mission continuity. Examples include the space missions FUSE [7], Dawn [8], Hayabusa [9], the Neil Gehrels Swift Observatory [10, 11], and the Kepler Space Telescope [12]. Failures originating from the AOCS system account for approximately 32% of all mission failures, according to [2], though it has to be noted that this percentage includes a broader range of failure modes beyond just reaction wheel issues.

To address these challenges, this paper explores a novel proof-of-concept torque generation system with a minimal number of mechanically moving parts, aiming to reduce solid-solid interfaces and avoid tribological degradation. Such a system would offer significant benefits for space missions requiring enhanced reliability and reduced maintenance demands.

This research investigates an alternative technological approach utilizing ferrofluids-liquids responsive to magnetic fields-to create a liquid–solid interface acting as a bearing in a system analogous to a reaction wheel. Ferrofluids consist of a carrier liquid containing magnetic nanoparticles in stable suspension, making them manipulatable via magnetic fields [13]. By utilizing ferrofluids and permanent magnets as bearing, it is possible to minimize the number of moving elements in the system [14–17].

This paper presents the development, in-space verification, and current state of the novel reaction wheel system, highlighting its potential for future space applications.

1.1 The FARGO project

The Überflieger 2 competition was organized by the German space agency within DLR and the Luxembourg Space Agency in 2020 with Yuri GmbH, SpaceTango, and the DPG (German Physical Society) as co-organizers. Among three other student teams, FARGO was selected as a winning student experiment proposal.

The selected student teams were given the opportunity to design, test, verify and finally operate their experiments for in-space verification on-board the ISS. The platform was a 2U TangoCube by SpaceTango, selected requirements for this experiment type are given in Table 1 and in the respective ICD in [18]. The experiments were operated in ISS microgravity for approximately one month in March and April 2023. The FARGO project consists of three different proof of concept experiments for mechanically-reduced ferrofluid technologies [19–21], two different types of switches and a reaction wheel variant. This paper is focused on the discussion of the latter. This experiment is from here on referred to as *Ferrowheel* as it is a ferrofluid based substitution for a reaction wheel. A selection of relevant requirements for the Ferrowheel suited to yield a proof-of-concept with FARGO is given in Table 2.

2 Ferrowheel system design

The Ferrowheel investigated in this study is classified as a BLDC outrunner, where the rotor is positioned externally, and the stator is located at the center. The system comprises a commercial off-the-shelf (COTS) BLDC stator, a corresponding controller, a custom made solid steel rotor disk, and a containment housing for the rotor, as illustrated as concept and model in Fig. 1.

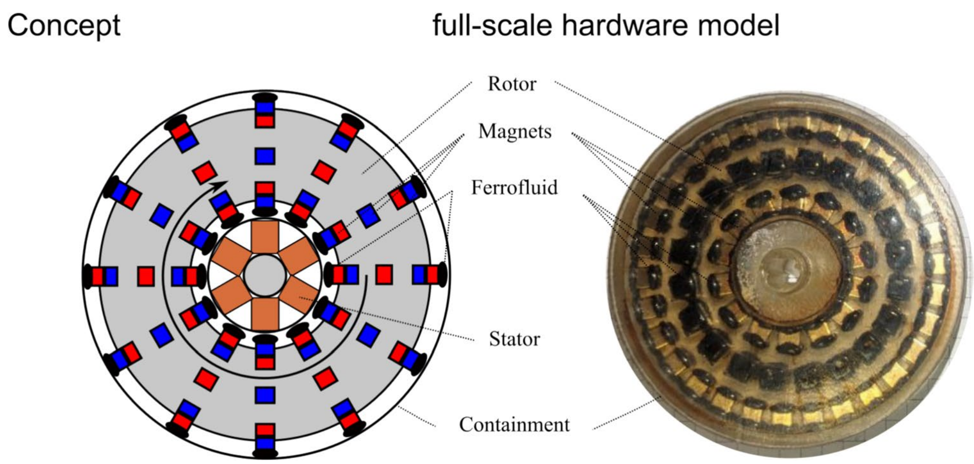

Fig. 1 Left: Ferrowheel concept drawing. Right: Full-scale functional FARGO Ferrowheel bearing model. The concept shows the principle of magnetisation and the respective alternating magnetic pairs for each ring of magnets as well as radially. Rotor, permanent magnets, application of ferrofluid and containment indicated. The model on the right is geometrically identical to the Ferrowheel flown on FARGO. The model is missing the stator core for full functionality

Table 1 Requirements FARGO

Shall operate in the ISS interior environment.
Shall fit within a 2U container ($20 \times 10 \times 10$ cm).
Shall not exceed a total mass of 2 kg.
Shall not include hazardous, explosive, or flammable materials.
Shall operate at 12 V with a power consumption of less than 12 W.
Shall operate autonomously, requiring no astronaut intervention.
Shall use UART for telemetry and USB for data transfer.
Shall withstand mechanical loads from launch, reentry, and transport.

Table 2 Selected Requirements Ferrowheel

Shall require less than 1 U of the experiment volume.
Shall have a fluid containment diameter of less than 8 cm.
Shall generate internal torque using a ferrofluidic system.
Shall operate with up to 2000 RPM.
Shall be able to measure torque of 0 to 100 mNm.
Shall resolve torque measurements within 0.1 to 1 mNm.
Shall maintain stable rotational operation during testing.
Shall use a second rotating system to mitigate torque impacts on the ISS.
Shall hermetically seal the ferrofluid to prevent leakage or contamination.
Shall allow visual observation of the rotor and ferrofluid behavior through a transparent containment lid.
Shall not exceed internal temperatures of more than 80°C during operation.
Shall have negligible external magnetic effects at any point.

The rotor disk, precision laser-cut from magnetic steel, features pockets specifically designed to hold 5 mm neodymium-iron-boron (NdFeB) permanent magnets. The choice of magnetic steel simplifies the assembly process, as the magnets naturally adhere to the pockets during placement. Epoxy adhesive is then applied to secure the magnets permanently. Each ring of alternating permanent magnets serves as a critical component of the ferrofluidic bearing, supporting a specific load direction once wetted with ferrofluid.

The radial forces in the Ferrowheel are managed by the innermost magnet ring, located at the stator, and the outermost magnet ring, positioned along the outer containment wall. While having two radial bearing rings is redundant in principle, it was deemed necessary for this design. The innermost ring is critical for establishing magnetic coupling between the rotor and stator, while the outermost ring, with its larger number of magnets, provides additional bearing forces to ensure smooth and stable operation.

The middle magnet ring is responsible for supporting axial loads and preventing rotor tilting. All permanent magnets in the Ferrowheel are coated with ferrofluid EFH-1, chosen for its high saturation magnetization, which enhances bearing load capacity, and its low viscosity, which minimizes friction losses [22].

The critical effect exploited in this system is the magnetic pressure experienced by the nanoparticles within the ferrofluid when subjected to a magnetic field [13]. This pressure, analogous to the static pressure in a liquid column within a gravitational potential field, arises from the attractive interaction between the ferrofluid's superparamagnetic properties and the magnetic potential field. The containment consists of two parts. The outer structure of the Ferrowheel is fabricated from milled PTFE and consists of two chambers: one for the rotor and the other for the stator. Additionally, the assembly includes a steel plate with a shaft interface, to be placed in a rotating frame.

The ferrofluid-wetted rotor is housed in the outer chamber of the main structure. This chamber is additionally filled with a secondary, non-magnetic fluid-a mixture of water and ethanol [20]-to eliminate air bubbles and enable clear observation during operation. Using air or another gas as the chamber filling would have led to significant surface staining by the ferrofluid, hindering observation. The carrier liquid, an opaque oil, combined with the high surface energy of the magnetic nanoparticles, tends to stain most surfaces quickly. To facilitate observation, the containment is sealed with a laser-cut transparent polycarbonate (PC) lid, allowing for unobstructed monitoring during experiments.

The BLDC stator is installed in the inner chamber. It is operated like a conventional BLDC motor with three-phase AC. Such a device produces a dynamic rotating magnetic field, causing reactive motion in the rotor by coupling to the alternating permanent magnets.

The Ferrowheel experiment design is shown as CAD model of the rotor itself, as well as the actual flight model setup as part of the FARGO experiment hardware in Fig. 2.

The second structural part is a steel plate with an shaft interface to increase the moment of inertia of the outer housing of the experiment. serves further as heat dissipation component of the occurring thermal loads of the BLDC stator into the structure. The Ferrowheel containment structure, shown in Fig. 3, is designed to rotate and is connected to the FARGO on-board computer via a slip ring for power and data transmission. This counter-rotating structure mitigates the impact of torque generation on the ISS and serves as a surrogate for a satellite. Its ability to rotate along its axis effectively simulates the reactive movement of a satellite in response to internal torque generation. A cross-sectional CAD model of the full FARGO Ferrowheel experiment setup is presented in Fig. 3.

The structure of the Ferrowheel experiment is depicted as a section cut in Fig. 3. Two mechanical bearings, positioned at the upper and lower ends, enable smooth rotational movement of the Ferrowheel containment within the FARGO experiment. Power and data are transferred from the static FARGO hardware interface to the rotating experiment hardware via a slip ring. Consequently, the total loss torque is the combined result of friction from the bearings and the slip ring.

The Ferrowheel containment is secured within a precision frame in the FARGO experiment using an aluminum shaft to ensure accurate encoder positioning. The relative rotation of the Ferrowheel is measured by attaching the encoder sensor

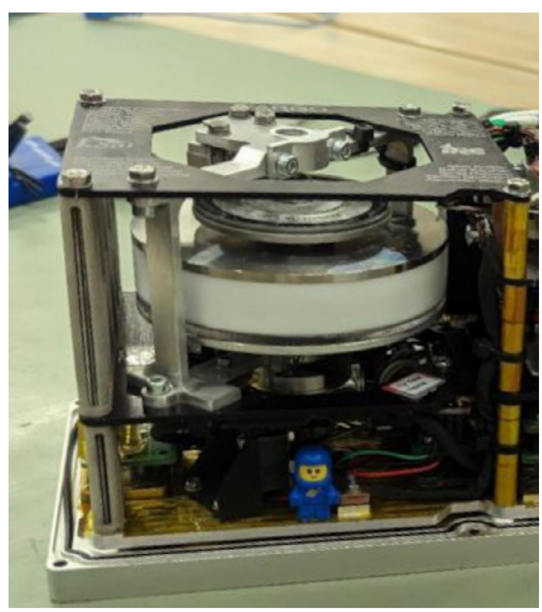

Fig. 2 The FARGO flight model setup, where the Ferrowheel is visible from the side perspective as white disk

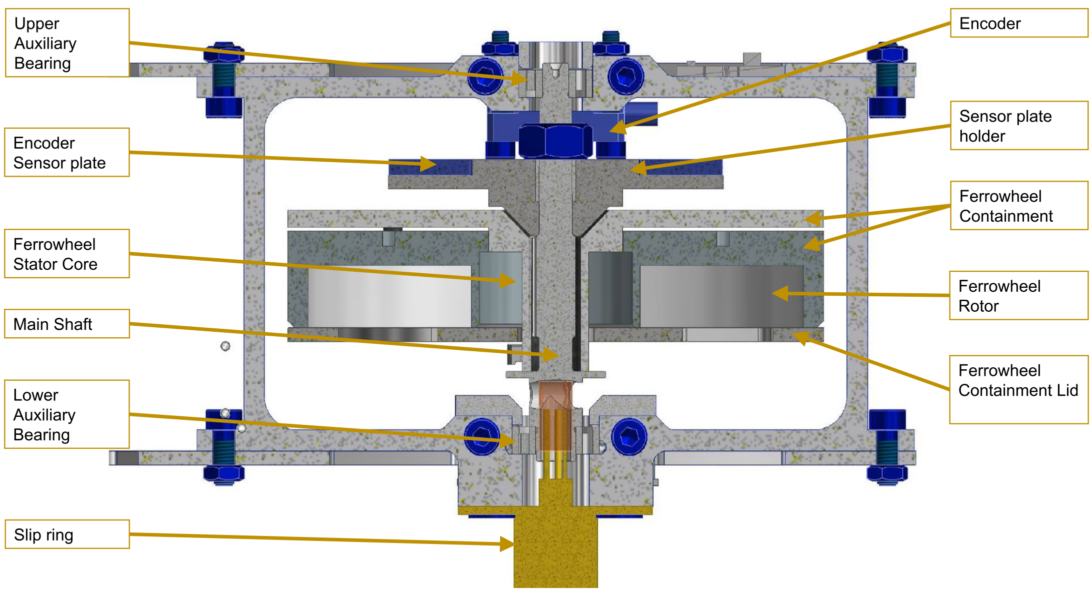

Fig. 3 Cross-sectional CAD model of the FARGO Ferrowheel experiment setup. The rotating assembly is visible along the central axis, including the AOCS main containment, auxilliary bearings, slip ring, sensor plate, and associated structures. The static structure, depicted as the outer grey frame, is fixed to the encoder, which measures the relative rotational movement of the outer containment

plate to the Ferrowheel containment, while the encoder itself is mounted on the precision frame. The outer containment achieves counter-rotation through the conservation of momentum when the internal Ferrowheel disk is accelerated.

The electronic-speed controller as well as the dedicated custom PCB are situated on the FARGO on-board computer and are therefore not shown.

To quantify the experiment performance during operation the following sensors are implemented: an incremental rotational encoder, a Hall sensor, a one-wire temperature sensor as well as a Raspberry Pi camera for visual observation. Additionally a dashboard of the payload hoster SpaceTango provides time resolved current and voltage data from the full FARGO experiment measured by the respective experiment rack on the ISS. As experiments are not executed in parallel the displayed current and voltage progression can be used to infer the state of the experiment and hardware to a limited degree.

As shown in Fig. 3, the sensor plate of the encoder is mounted on the containment and the encoder read-head on the frame. The one-wire temperature sensor as well as the Hall sensor is attached to the frame, the position is indicated in Fig. 4.

An in-depth system design description and fundamental information on the operating principle of the FARGO Ferrowheel and physics of reaction wheels is given in [23].

The presence of liquids in the Ferrowheel system (i.e., ferrofluid and the non-magnetic secondary liquid) introduces potential challenges related to outgassing and outgassing during spaceflight. For practical applications, the secondary liquid is not required, leaving the long-term evaporation of the ferrofluid as the primary concern. In the FARGO experiment, EFH-1 ferrofluid-a light hydrocarbon-based fluid-was used [22]. While EFH-1 is prone to evaporation and drying under ambient conditions, these effects could pose significant challenges in a vacuum environment. To address this, the liquid-containing component of the Ferrowheel can simply be fully sealed, and achieving hermetic tightness effectively mitigates outgassing issues. Additionally, maintaining an inert gas environment inside the containment at a pressure above the ferrofluid's evaporation threshold could further preserve its integrity. However, the presence of an inert gas may introduce high aerodynamic drag losses,

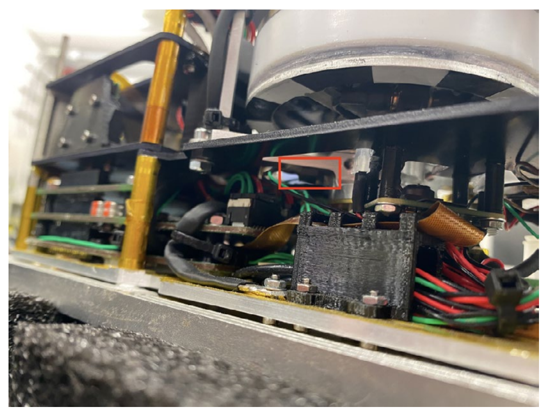

Fig. 4 Position of the one-wire temperature sensor and Hall Sensor of the FARGO Ferrowheel experiment

potentially affecting the system's efficiency in space applications—especially at high speeds. Alternatively, vacuum-compatible ferrofluids, commonly used in vacuum chamber feedthroughs [24], offer a viable solution. However, no experience or heritage currently exists regarding their viscosity and the associated friction losses in this context.

3 Ferrowheel operation

The Ferrowheel experiment was tested under various conditions, including ground testing, in-orbit operation aboard the International Space Station (ISS), and limited post-flight evaluation. Each phase of testing provided critical insights into the system's behavior, performance, and potential limitations. This section outlines the three key stages of the Ferrowheel's operational testing: preparation through ground testing, execution of the in-orbit experiment, and post-flight analysis to assess the long-term integrity and performance of the system.

3.1 Preparation: ground testing

The Ferrowheel experiment was developed in a fast-paced environment, with less than 14 months of total development time from the initial concept submission to the space agency within DLR agency, subsequent selection and then launch to the International Space Station (ISS). This compressed schedule necessitated a rapid, iterative design process to determine a working geometry and ensure compliance with the strict volume constraints of the 2U payload container, as well as the power requirements of the onboard systems given by SpaceTango.

Preparatory testing focused on successively evaluating the performance and suitability of individual components and configurations. For the final design, multiple sessions of manual iterative testing were required to determine the startup parameters for the electronic speed controller (ESC). While the stator is a commercial off-the-shelf (COTS) component, the rotor is custom-built, introducing additional challenges. This non-standard configuration made it difficult for the ESC to initiate rotor startup and transition reliably to a constant RPM mode. Achieving this required manual tuning of startup ramp parameters, including target RPM, ramp duration, and maximum allowable current.

During the determination procedure of these ramp parameters the system exhibited intermittent reliability issues: the ESC parameters enabled successful startups and continuous operation on some occasions but failed to do so consistently. The root cause of this unreliability remained unclear at this point.

After extensive effort, a final set of startup parameters was identified and verified through repeated ground tests to ensure consistent performance. This included ground tests at the Kennedy Space Center after shipping the flight hardware to the launch site. The setting of the ramp parameters was critical as in-orbit adaptation of these parameters was not possible due to the limitations of the ESC interface used in the experiment.

3.2 Execution: in-orbit testing

Various experiments and test were performed to validate the functionality of a ferrofluid-bearing reaction wheel in space.

As a Raspberry Pi cam was part of the experiment, a collage of recorded visual data is given in Fig. 5. Here, the typical behavior observed during the startup of a Ferrowheel experiment, divided into four distinct phases, is shown.

Phase one depicts the experiment in a pristine—i.e. clear viewable—state before any operation [25].

In phase two, limited staining of the ferrofluid is observed on the experiment transparent wall, validating the design choice of employing a non-staining secondary liquid. The lack of clear resolution of the ferrofluid-wetted rim indicates movement, which is in agreement with the created light-stain ring of ferrofluid slightly offset to the central axis of rotation.

Phase three demonstrates that at sufficiently high RPM, the ferrofluid begins to relocate by creating streams of ferrofluid. Interestingly, the movement is directed inward, which is counterintuitive, as one would typically expect an outward motion due to centrifugal forces. This inward motion is likely attributed to the formation of a vortex cell, induced by the high velocity along the outer containment wall and the lower relative velocity at the inner containment wall. No detrimental effects have been observed due to this liquid relocation.

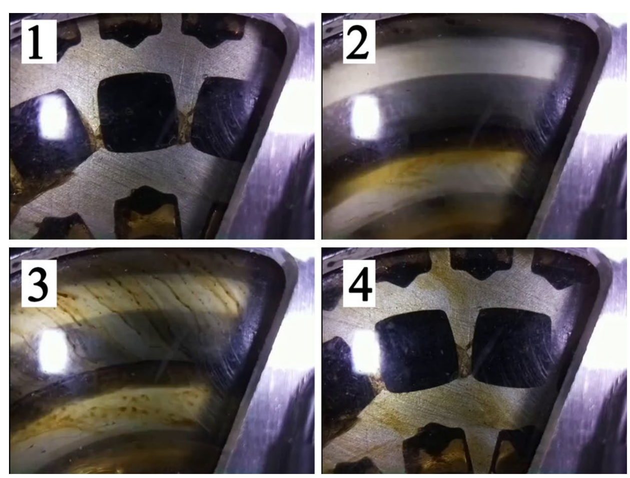

Fig. 5 FARGO Ferrowheel in-space recording during startup via Raspberry Pi cam in four typical phases. 1) stand-still (exemplary), 2) spin up, 3) spinning with ferrofluid relocation, 4) immediate state at sudden stop [25]

Phase four, following experiment termination, closely resembles phase one. Only minor liquid relocation effects are observed, suggesting that this type of Ferrowheel design exhibits an expected self-resetting behavior. Minor stains will over time disappear by merging the staining-ferrofluid with the existing ferrofluid-cushions at the permanent magnets.

In the following, a discussion on non-optical sensor data is given. The Hall sensor measures magnetic field strength and temperature, the one-wire sensor measures temperature and the encoder measures counts with a time stamp, corresponding to angular increments. The first and second derivatives of this yield angular velocity and angular acceleration. In addition, the current consumption data of the dashboard is available, see Fig. 6.

In a first fundamental test, the basic functionality of the Ferrowheel and the sensors was checked after arriving at the ISS. For this purpose, the Ferrowheel was accelerated to a target rotation rate of 800 RPM.

The current data on the dashboard in Fig. 6 indicates the Ferrowheel experiment startup and subsequent termination after approx. 10 min of experiment operation.

This can be seen in Fig. 6 as the current increases to 1.28 A during the start-up phase. During the transition attempt to continuous operation, the current drops to 0.78 A. After 288 s, the current drops from 0.78 A to 0.72 A. It is highly likely that here the rotor came to a full stop as the controller was unable to perform the transition from open loop control during startup to closed loop (field oriented) control in continuous operation mode. It is unclear why such a high power draw was still given, which would be consistent with continued operation. The BLDC switched off after 850 s. The power required during start-up is 15.35 W and during the attempted continuous operation 8.66 W. The Hall sensor measures the magnetic field strength in three directions over time as graphed in Fig. 7.

At the time step of the amplitude change seen at around 155 s in Fig. 7 the Ferrowheel is switched on and subsequently the experiment switched off after 850 s. While all three axis show an increase in magnetic field amplitude, it is most significant in z-direction, due to its relative position of the sensor to the experiment. The maximum magnetic field strength measured by the Hall sensor is 0.35 mT in the x-direction in a distance of 19 mm in air. Such magnetic field strength are considered sufficiently low that EMI is unlikely for this design. No EMI effects were observed during FARGO's operation. To validate the thermal behaviour, the temperature was measured by a one-wire sensor and a temperature sensor that was part of the Hall Sensor component. Figure 8 shows the progression of both sensors over time.

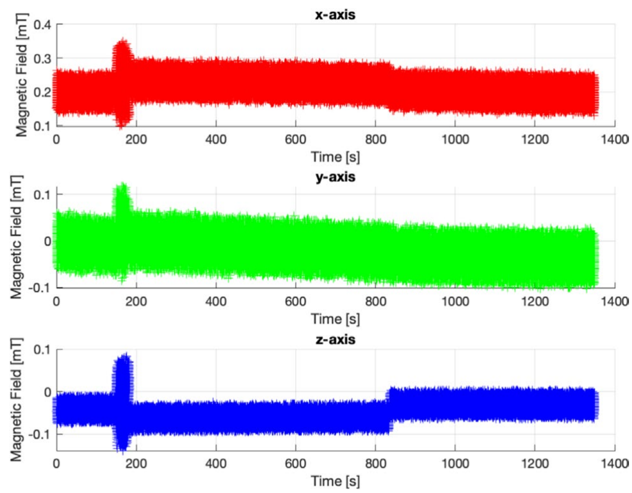

Fig. 7 FARGO Ferrowheel experiment Hall sensor recording, experiment start at approximately 155 s

The temperature curves shown in Fig. 8 are offset to each other. The main reason for this is that the one-wire sensor is attached directly onto the frame. Furthermore, it can be seen that the temperature increases sharply after 155 s. This is consistent with the Ferrowheel experiment being started. The BLDC stator core heats up the entire system. The maximum temperature reached is 35.6 °C at the one-wire sensor and 30.8 °C at temperature sensor of the Hall sensor package.

Due to the thermal stability of PTFE, a maximum temperature of 80 °C was set at the one-wire sensor for all

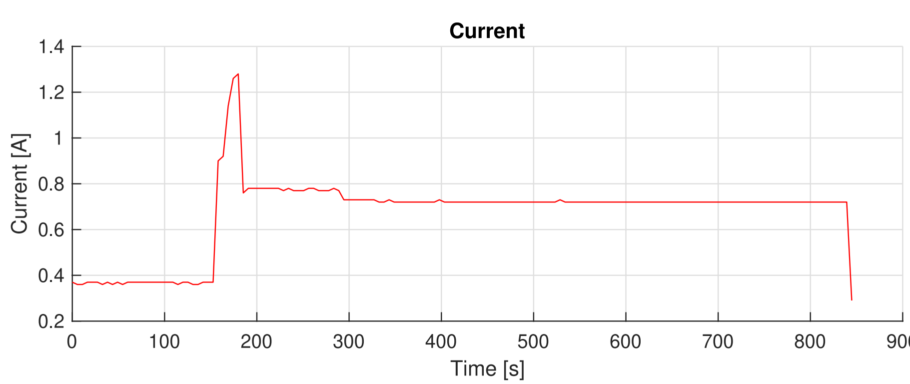

Fig. 6 FARGO Ferrowheel experiment payload dashboard recording of experiment power draw @12V nominal voltage during function check

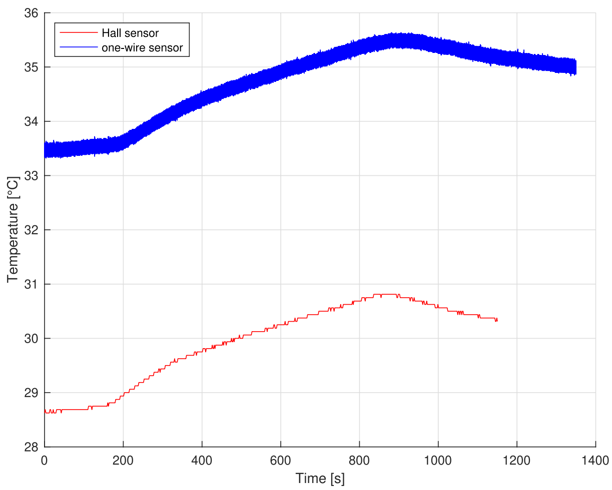

Fig. 8 Temperature progression graph for the Hall sensor in red and the one-Wire sensor in blue. Experiment activation at approximately 155 s

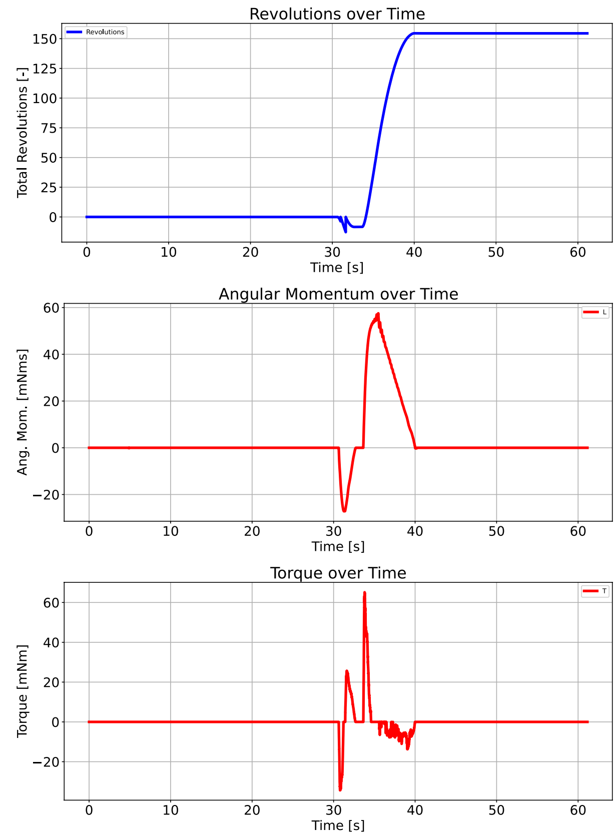

Fig. 9 FARGO Ferrowheel experiment external frame encoder readings as revolutions as well as the integration to angular momentum and torque. The external frame quickly stops after startup

experiments, emergency shutdown is automatically triggered when this temperature limit is exceeded.

After switching off the Ferrowheel BLDC, the temperature at the one-wire sensor drops to 34.8 °C within 500 s. The temperature gradient flattens with increasing experiment duration. This indicates that after a certain experiment time the Ferrowheel reaches thermal equilibrium. Due to a software error the encoder did not generate data during this experiment, subsequent software updates were developed and implemented.

In a second encoder test experiment, the angular momentum and torque of the Ferrowheel were determined for a rotation rate of 800 RPM of the rotor disc. The Ferrowheel was commanded to be accelerated to 800 RPM. After 1776 s, the experiment was reset due to not stopping the experiment autonomously for unknown reasons. Consequently the sensor recordings were interrupted by this event.

The encoder data in Fig. 9 show that the Ferrowheel accelerates to 800 RPM and then no further encoder increments of a rotating external structure is counted for 1776 s.

The Ferrowheel operation of experiment generates for the outer frame an angular momentum of $L = 59\,\mathrm{mN\,m\,s}$ and a torque of $T = 65\,\mathrm{mN\,m}$. It has to be noted that the external frame behaviour and the internal rotating disc behave different over time, while the rotor discs continues to rotate the external frame does loose its angular momentum via friction of bearings and the slip ring to the environment, i.e. the ISS). At the same time, the stator or the respective controller is attempting to keep the rotation rate of the rotor at constant target velocity. The current progression of the dashboard in Fig. 10 is similar to the current graph of the previous experiment with a maximum of $I_{\mathrm{start}} = 1.34$ A during start-up and $I_{\mathrm{cruise}} = 0.78$ A during the continued activation of the BLDC stator, while the controller likely failed to achieve the transition between startup and continuous mode.

After 1776 s, a reset of the Ferrowheel experiment was executed. The current drops to 0.03 A and the entire Ferrowheel experiment shuts down. The power required during start-up is $P_{\mathrm{start}} = 16.55$ W and during continuous operation $P_{\mathrm{cruise}} = 9.38$ W. When starting up the Ferrowheel the Hall sensor data in Fig. 11 show a maximum measured magnetic field strength of 0.61 mT.

The first discussed experiment had duration of approximately 7.5 min, while this experiment lasted almost 30 min impacting the thermal behaviour. The temperature graph in Fig. 12 shows that the temperature of the one-wire sensor reaches 37.11 °C and the temperature of the temperature sensor within the Hall sensor reaches 31.6 °C.

The subsequent cooling phase could not be recorded due to hardware reset and, therefore, the off-state of the sensors.

In the last experiment discussed in this paper, the continuous operation at a higher speed was attempted as well as the thermal behaviour of the system. For this purpose, the Ferrowheel was accelerated to 1000 RPM.

Fig. 10 FARGO Ferrowheel experiment payload dashboard recording of experiment power draw @12V nominal voltage during 800 RPM target velocity. Startup failed transition to continuous mode, continued operation of the BLDC stator of experiment

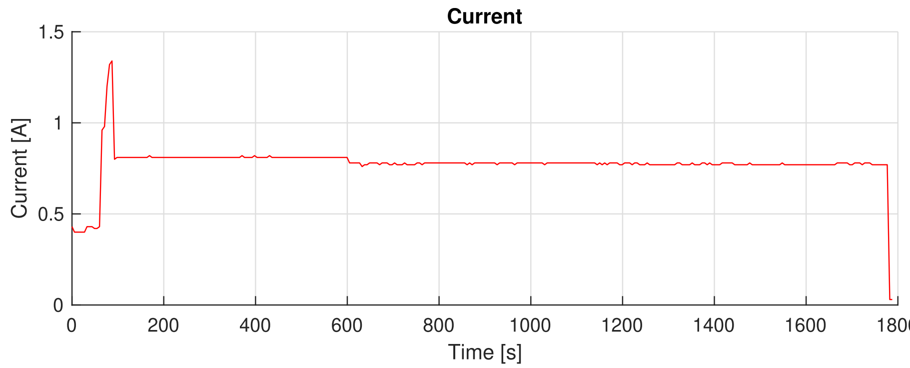

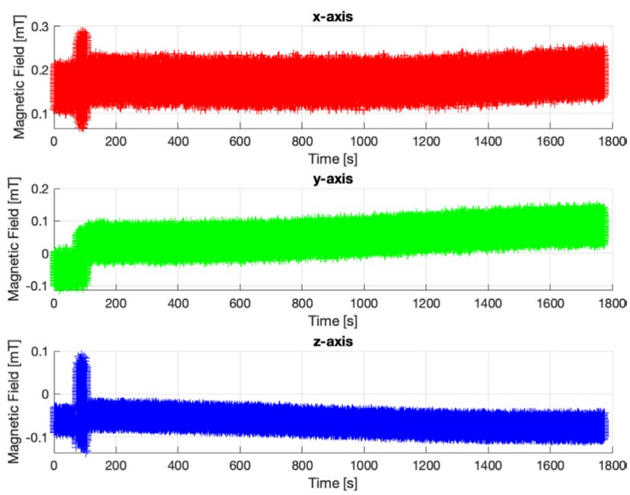

Fig. 11 FARGO Ferrowheel experiment Hall sensor recording during 800 RPM target velocity. Startup failed transition to continuous mode, continued operation of the BLDC stator of experiment

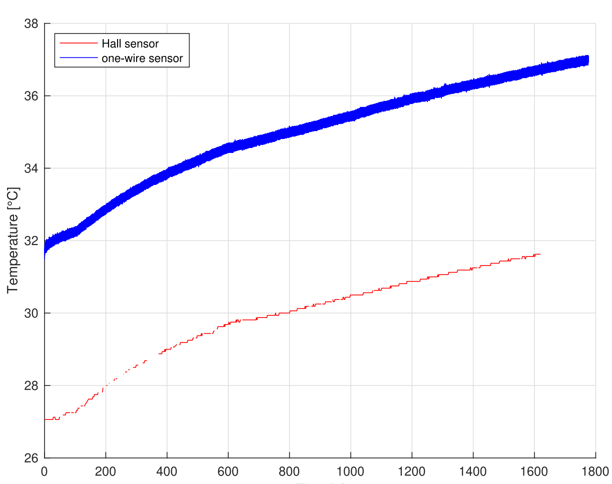

Fig. 12 Temperature progression graph for the Hall sensor in red and the one-Wire sensor in blue during 800 RPM target velocity. Startup failed transition to continuous mode continued operation of the BLDC stator of experiment

The current in Fig. 13 shows a drop to $I_{\text{post start}} = 0.69$ A from the maximum of $I_{\text{start}} = 1.38$ A after the start-up, before the current increases to $I_{\text{cruise}} = 0.97$ A.

This indicates that the start-up failed once more and the rotor of the Ferrowheel stopped immediately after the end of the start-up phase. Furthermore, the dashboard current indicates that the fault was not detected by the system and the BLDC generated a magnetic field for a target speed of 1000 RPM until the end of the test, even though the rotor stopped. The power required during start-up is $P_{\text{start}} = 16.55$ W and during continuous operation $P_{\text{cruise}} = 11.67$ W. The encoder data in Fig. 14 agrees with this assumption.

Here, it can be seen that the Ferrowheel produces an angular momentum of 67 mN m s and a torque of 65 mN m shortly after the start. As mentioned in the previous test, the outer frame also loses its angular momentum to the environment due to the friction of the bearings and the slip ring. After 1891 s, when the BLDC is switched off, there is no recorded change. The constant current flow and the assumption that the BLDC continues to generate a magnetic field coincides with the data from the Hall sensor in Fig. 15, which registers the rotating magnetic field of the BLDC by the change in amplitude from 74 s to 1891 s.

The activation of the FARGO BLDC stator can be seen in the temperature data of the Hall sensor in Fig. 16.

The temperature steadily increases as the BLDC is active. The maximum temperature reached is $T_{\max} = 41.3$ °C at the temperature sensor within the Hall sensor. Likely due to a software fault, the temperature of the one-wire sensor was not available for this experiment. It can be assumed that it was higher than the Hall sensor, as is consistently seen in Fig. 8 and Fig. 12. The temperature curve shows a strong gradient, therefore thermal equilibrium has not been reached yet.

After 5706 s, a restart of the Ferrowheel with a target rotation rate of 1200 RPM was attempted. This resulted in triggering an internal fuse due to over current causing a system shut down. The current peak in Fig. 13 was $I_{\text{peak}} = 1.72$ A. The Ferrowheel start attempt also explains the increase in amplitude of the Hall sensor and encoder

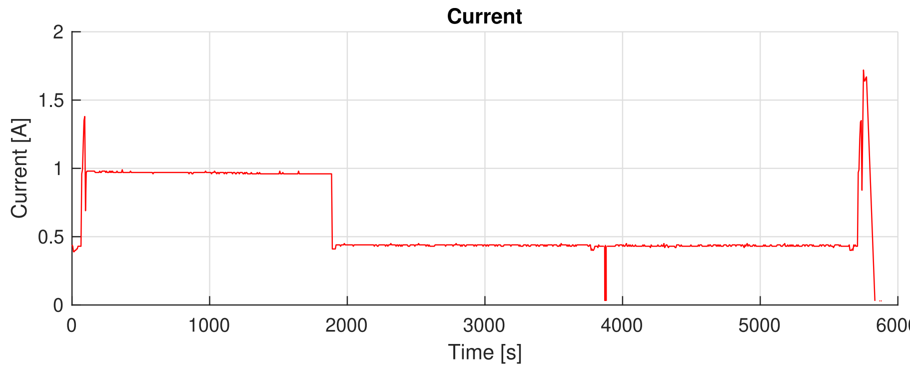

Fig. 13 FARGO Ferrowheel experiment payload dashboard recording of experiment power draw @12V nominal voltage during 1000 RPM experiment

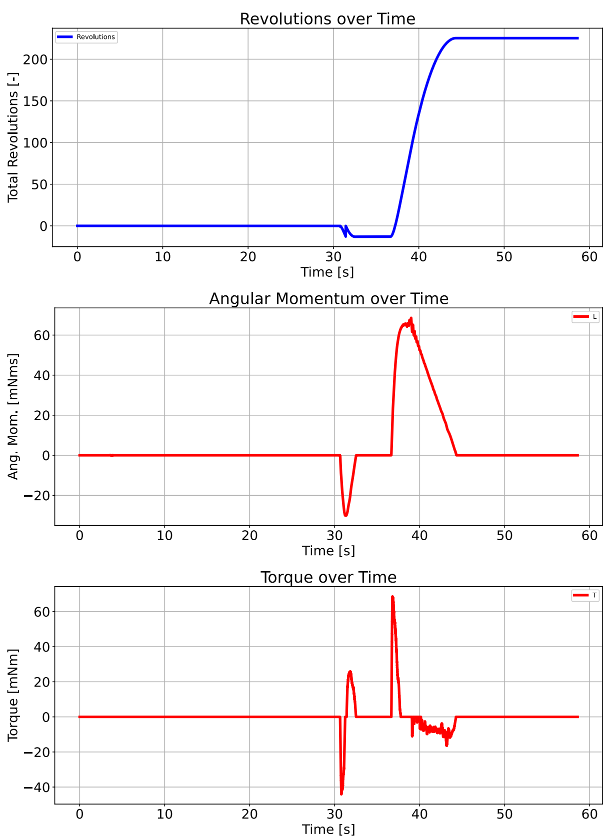

Fig. 14 FARGO Ferrowheel experiment external frame encoder readings as revolutions as well as the integration to angular momentum and torque during 1000 RPM experiment

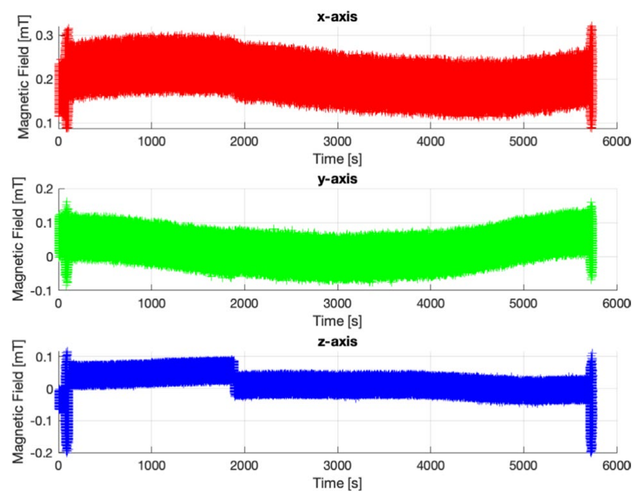

Fig. 15 FARGO Ferrowheel experiment Hall sensor recording during 1000 RPM target velocity. Startup failed transition to continuous mode, continued operation of the BLDC stator of experiment

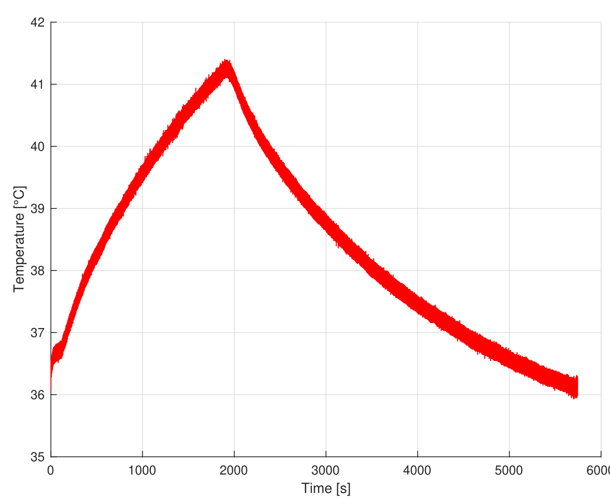

Fig. 16 Temperature progression graph for the Hall sensor in red during 1000 RPM continued operation experiment

reading after 5706 s. Due to the fuse triggered termination, no further data could be collected.

Through these experiments, along with the consideration of encoder data, a correlation between experiment function and supply current becomes evident.

Thus, first limited insights into in-space function and performance for this design of Ferrowheel is achieved through the testing campaign of FARGO on the ISS.

3.3 Post-flight testing

After the return of the FARGO hardware, limited post-flight analysis and testing were conducted. The hardware was inspected for damage using a computed tomography (CT) scan at the DLR facility in Stuttgart. The results confirmed that no damage to vital experiment components occurred during the return to Earth or subsequent shipping to Germany.

A limited investigation into the previously observed anomalous behavior was also performed. Despite the issues encountered in orbit, the Ferrowheel was able to start successfully during post-flight testing. This demonstrated that the ferrofluidic bearing and attitude control mechanisms had endured the mechanical loads associated with reentry and transportation. Furthermore, the persistence of the electronic speed controller (ESC) issue—its inability to transition into continuous operation mode—even under ground conditions indicates that the anomaly is most likely not caused by the space environment but instead related to the hardware or control parameters.

A potential root cause for the anomaly may lie in the inherent system design. The electronic speed controller (ESC) executes its startup procedure based on its internal algorithm, which is designed for sensorless BLDC stators. In such configurations, the rotor's position is inferred from the back electromotive force (back-EMF) generated in the three-phase AC leads as the permanent magnets of the rotor pass the stator coils.

During startup, the ESC may successfully execute its procedure nominally. However, the frictional losses from the ferrofluidic bearing and the slip ring could be sufficient to prevent initial rotor motion, leaving the system static. Once the slip ring overcomes static friction and begins to move, the stator as part of the outer containment will rotate in the opposite direction of the rotor's intended motion. From the perspective of the ESC, which interprets this motion as part of the static system, this could appear as a sudden, anomalous spike in RPM. Such a perceived spike may potentially disrupt the controller software, causing it to crash or fail to complete the transition to continuous operation mode. Additionally, the specific frictional characteristics of the slip ring could vary due to ambient environmental conditions, such as temperature and pressure, as well as the thermal effects of prior operation. These variations may contribute to observed inconsistent behavior, with the system sometimes performing reliably and at other times requiring manual adjustment of startup parameters. This variability underscores the need for a more robust startup algorithm or hardware adaptations to mitigate such inconsistencies.

Further modifications to the hardware or extensive testing were not pursued, as the Ferrowheel is heritage flight hardware and must be preserved in its post-mission condition. The FARGO module is now a valued exhibit used for STEM outreach and engagement. It is frequently showcased by the University of Stuttgart, the Institute of Space Systems, and the student society KSat e.V., serving as an effective tool for inspiring future generations to pursue STEM in general and consider space systems engineering in particular.

4 Conclusion

Mechanical reaction wheels have been a cornerstone of spacecraft attitude control, delivering exceptional reliability across a wide range of spacecraft and mission profiles with several decades of heritage. This paper introduced and explored a novel concept: the ferrofluid-based reaction wheel (Ferrowheel), which aims to eliminate key mechanical weak points by incorporating ferrofluidic bearings, enabling smoother and potentially more durable operation.

A prototype validated the viability of the ferrofluid bearing which has been tested on the ISS. The concept of the Ferrowheel is explained, and its in-space performance is assessed where possible. Key design considerations and the analysis of data from the in-space tests are given. To summarize the FARGO Ferrowheel experiment operation: multiple startup attempts with target speed of 800 and 1000 RPM were made respectively. The controller was unable to transition from startup mode to continuous control mode. Nonetheless, power draw and respective heat dissipation was similar to a successful operation. The experiment did not exceed a temperature of 42 °C, although the experienced modes can be considered an operational worst case.

Basic functionality of the design was shown by repeatedly rotating the Ferrowheel during startup, while extended operation was not achieved. During this startup, a peak torque of $T = 65\,\mathrm{mN\,m}$ was derived from encoder measurements. The potential of EMI has been addressed and is considered negligible, even without magnetic shielding. The Ferrowheel successfully generated torque strong enough to rotate the outer containment, with the rotation rate electrically controlled. The ferrofluidic bearing demonstrated flawless performance, with the suspension system-relying on permanent magnets-proving viable under the forces encountered. During operation, the ferrofluid redistributed under load, but this change was uniform and had no adverse impact on performance. The reliability of the controller, controller software and Ferrowheel startup is still a relevant challenge with the current system design as well as the associated heat generation and dissipation. This could be counteracted with a cooling system in case of need. In order to keep up with conventional systems, the required power of the system must be reduced, i.e. the efficiency of the magnetic coupling from stator to rotor has to be improved. One point of optimisation would be to reduce the air gap between the BLDC stator and the ferrofluid wetted rotor in order to be able to generate similar forces accelerating the rotor with less current due to the increase in magnetic field strength. Another option for improvements are geometric of material selection changes to the bearing design itself, to reduce friction and system complexity. In conclusion, a ferrofluid-based RW—like the shown Ferrowheel design—have the clear potential to replace conventional RWs to enable a more robust and reliable future of space flight. At the moment, the tested Ferrowheel prototype cannot yet perform speeds comparable to conventional RW systems (i.e. 5, 000 - 20, 000 RPMs), but the results provided show a promising path toward competitiveness. It should be noted that conventional RW systems have long standing heritage and are considered highly reliable, making them one of the current state of the art solution for spacecraft attitude control. Achieving competitiveness with these established systems will require further development and refinement of the Ferrowheel. However, the progress achieved within less than 1.5 years through a student-led project-including successful testing aboard the ISS-demonstrates the feasibility and promise of ferrofluid-based systems at least as a complementary technology for niche applications requiring reduced mechanical interfaces, smooth operation and enhanced durability.

5 Outlook

As with any innovative technology, further work remains to fully realize its potential. For the FARGO Ferrowheel, additional testing and iterative concept revisions are essential to refine its design and enhance its performance. Since the experiment payload had a limited mission duration on the ISS, it is recommended to conduct endurance testing for several weeks, or ideally, for months. Due to ISS operational safety considerations and the power draw of the payload card, the speed was limited during operation. It is crucial to assess the Ferrowheel's behavior across its entire performance range, including the permitted minimum and maximum speed, as well as its performance during directional changes (i.e., over the 0 RPM point). This assessment is vital for the future deployment of this innovative component.

As operation and startup of the Ferrowheel with off-the-shelf BLDC controller kits proved itself challenging it is important to invest additional time to either correctly adapt the COTS controller for effective and reliable operation or create a custom controller for this use case. When creating a custom controller it is simpler to already include fully space-qualified components than adapting a COTS component.

Beyond the current—verified—design of the Ferrowheel the next iteration will be focused on a simplification in terms of part count and integration effort [25]. For this new design, the mosaic like pattern of three distinct rims of magnets bearing the Ferrowheel will be replaced.

A new version is likely to be equipped with one or two torus magnets that can be integrated central around the rotation axis. Torus magnets wetted with ferrofluids can bear axial and traversal loads at the same time. The round surface of torus magnets permits even smoother operation, while integration 1 or 2 torus magnets requires significantly less effort that the 50+ cuboid magnets that had to be carefully arranged for the FARGO Ferrowheel. As this new concept requires no outer rim of bearing magnets it is possible to add various fly wheel designs to the rotor base, allowing for simple design adaption to accommodate specific mission needs for rotational momentum storage.

As the technology is promising and relatively simple to scale and adapt to various missions the Ferrowheel is currently planned as part of upcoming cubesat missions of the Institute of Space Systems of the University of Stuttgart. With this an increase in TRL up to 8/9 is possible as a dedicated mission provides the correct environment for this component. Although, this would make the ferrofluid still a experiment payload on the CubeSat it is important to note that synergy with other payloads that have requirements in terms of attitude, rotation rate or torques exists.

Acknowledgements The Ferrowheel experiment within the FARGO project was made possible through the support of German Space Agency at DLR as part of the Überflieger 2 competition (Grant No. 50WF2001). We extend our sincere gratitude to DLR, the German Physical Society (DPG), the technical advisors at Yuri GmbH, the payload operators at SpaceTango, and all contributors who generously dedicated their time and resources to the FARGO project. We also wish to thank the Institute of Space Systems at the University of Stuttgart for their academic supervision. Additionally, we acknowledge the invaluable contributions of the student association KSat e.V., whose members-both within and beyond the FARGO team-demonstrated exceptional dedication and support throughout the past two years. Furthermore, we recognize the FerrAC project (Ferrofluid Attitude Control, German Space Agency at DLR Grant No. 50RK1973), from which the initial concept and preliminary development of the Ferrowheel originated. Finally, we sincerely appreciate the reviewers' precise and constructive feedback, which has significantly contributed to improving this work.

Author contributions The FARGO project was a collaborative endeavor, with each team member playing an essential role in the experiment's conception, design, development, testing, and in-space operation. All authors contributed to the manuscript's review process, ensuring its accuracy and completeness.

Funding Open Access funding enabled and organized by Projekt DEAL.

Data availability Data is provided within the manuscript or supplementary information files.

Declarations

Conflict of interest The authors declare no conflict of interests.

References

1. Fusaro, R.L.: Nasa space mechanisms handbook: Lessons learned documented. (1999)
2. Tafazoli, Mak: A study of on-orbit spacecraft failures. Acta Astronaut **64**(2), 195–205 (2009). https://doi.org/10.1016/j.actaastro.2008.07.019. (**ISSN: 0094-5765.**)
3. Bialke, W. and Hansell, E.: A newly discovered branch of the fault tree explaining systemic reaction wheel failures and anomalies. (2017)
4. https://hubblesite.org/mission-and-telescope/servicing-missions
5. Andreoli, Claire: Nasa's hubble pauses science due to gyro issue - nasa science, Apr (2024). https://science.nasa.gov/missions/hubble/nasas-hubble-pauses-science-due-to-gyro-issue/
6. Claire A.: Hubble space telescope - gyroscopes https://science.nasa.gov/wp-content/uploads/2022/05/hst-gyro-fact-sheet.pdf?emrc=673f8b530b7b4 (2023)
7. Fuse frequently asked questions about reaction wheels, last accessed 21.11.2024. https://archive.stsci.edu/fuse/reports/RW_FAQ.html
8. Landau, E.: Dawn observing ceres; 3rd reaction wheel malfunctions, last accessed 21.11.2024. https://www.jpl.nasa.gov/news/dawn-observing-ceres-3rd-reaction-wheel-malfunctions/
9. Hayabusa, last accessed 21.11.2024. https://science.nasa.gov/mission/hayabusa/
10. Gohd, C: Nasa's gamma-ray observatory is in safe mode after a possible wheel failure, last accessed 21.11.2024. https://www.space.com/nasa-swift-observatory-safe-mode-reaction-wheel
11. Howell, E: Nasa's gamma-ray observatory is back in action after technical glitch, last accessed 21.11.2024. https://www.space.com/nasa-gamma-ray-observatory-back
12. Larson, K A., et al.: *Kepler Mission Operations Response to Wheel Anomalies*. https://doi.org/10.2514/6.2014-1882
13. Odenbach, S.: Ferrofluids. Magnetically Controllable Fluids and Their Applications. Springer-Verlag GmbH, Berlin (2002)
14. Ehresmann, M., et al.:Papell: solid-state pumping mechanism-Presented at Human Spaceflight and Weightlessness Science, Toulouse. (2018)
15. Ehresmann, M., et al., PAPELL: Mechanic-free Actuators through Ferrofluids: Presented at 12th IAA Symposium on Small Satellites for Earth Observation, Berlin. (2019)
16. Hild, F., et al., PAPELL: Final Student Experiment Design of a Non-mechanical Pumping System on the ISS: Presented at 69 th International Astronautical Congress IAC, Bremen. (2018)
17. Sütterlin, S., et al., FARGO -VALIDATION OF SPACE-RELEVANT FERROFLUID APPLICATIONS ON THE ISS; Presented at 71st DLRK Symposium, Dresden. (2022)
18. SpaceTango.https://ueberflieger.space/wp-content/uploads/2021/08/CubeLab-Interface-Control_Document-Rev2-1.pdf (2021)
19. KSat-e.V. Ferrofluid application research goes orbital, last accessed 21.11.2024. https://www.ksat-stuttgart.de/en/fargo-en/
20. Breitenbücher, L., et al., Assessment of ferrofluid interaction with secondary liquids;: Presented at 71st international astronautical congress, the cyberspace edition. (2020). https://www.researchgate.net/publication/344631176_Assessment_of_Ferrofluid_interaction_with_secondary_liquids
21. NASA. Überflieger 2: Ferrofluid application research goes orbital, last accessed 21.11.2024. https://www.nasa.gov/mission/station/research-explorer/investigation/?#id=8949
22. Ferrotec GmbH. Safety data sheet efh-1, last accessed 09.02.2023. https://ferrofluid.ferrotec.com/wp-content/uploads/sites/3/efhsds.pdf
23. Zajonz, S., et al.: Development of a ferrofluid-based attitude control actuator for verification on the iss. Aerotec Missili Spaz **103**(3), 303–314 (2024). https://doi.org/10.1007/s42496-024-00208-6
24. Ferrotec Material Technologies Corporation. Ultra high vacuum type, last accessed 21.11.2024. https://ft-mt.co.jp/en/product/semiconductor_equipment/ferrofluidics_seal/magnetic_fluid/multi/high_vacuum/
25. Ehresmann, M., et al.: An innovative wearless attitude control actuator based on ferrofluid manipulation tested on the ISS. *34th International Symposium on Space Technology and Science*, 6 (2023)